

Regional soil moisture retrievals and simulations from assimilation of satellite microwave brightness temperature observations

Xiaokang Shi · Jun Wen · Lei Wang ·
Tangtang Zhang · Hui Tian · Xin Wang ·
Rong Liu · Jinghui Zhang

Received: 9 July 2009 / Accepted: 15 February 2010 / Published online: 6 March 2010
© Springer-Verlag 2010

Abstract Low-frequency microwave satellite observations are sensitive to land surface soil moisture (SM). Using satellite microwave brightness temperature observations to improve SM simulations of numerical weather, climate and hydrological predictions is one of the most active research areas of the geoscience community. In this paper, Yan and Jins' (J Radio Sci 19(4):386–392, 2004) theory on the relationship between satellite microwave remote sensing polarization index and SM is used to estimate land surface SM values from the advanced microwave scanning radiometer-E (AMSR-E) brightness temperature data. With consideration of soil texture, surface roughness, optical thickness, and the monthly means of NASA AMSR-E SM data products, the regional daily land surface SM values are estimated over the eastern part of the Qinghai-Tibet Plateau. The resulting SM retrievals are better than the NASA daily AMSR-E SM product. The retrieved SM values are generally lower than the ground measurements from the Maqu Station (33.85°N, 102.57°E) and the Tanglha Station (33.07°N, 91.94°E) and the US NCEP reanalysis data, but the temporal variations of the retrieved SM demonstrate more realistic response to the observed precipitation events. In order to improve the land surface SM simulating ability of the weather research and forecasting model, the retrieved SM was assimilated into the Noah land surface model by the Newtonian relaxation (NR) method. A direct insertion

method was also applied for comparison. The results indicate that fine-tuning the quality factor in the NR method improves the simulated SM values most for desert areas, followed by grasslands, and shrub and grass mixed zones at the regional scale. At the temporal scale, the NR method decreased the root mean square error between the simulated SM and actual observed SM by 0.03 and 0.07 m³/m³ at the Maqu and Tanglha Stations, respectively, and the temporal variation of simulated SM values was much closer to the ground-measured SM values.

Keywords WRF · Noah · AMSR-E · Soil moisture

Introduction

Soil moisture (SM) is an important factor in global water and energy cycles. It controls the partition between the sensible and latent heat fluxes (Prigent et al. 2005) and the redistribution of rainfall into infiltration, surface runoff and evaporation on the earth surface (Vinnikov and Yezerepova 1991; Wagner et al. 2003). Thus, SM can influence the climate change by land–air interaction in the near surface layer (Clark and Arritt 1995; Gallus and Segal 2000). As a result, it is crucial to obtain an accurate SM field to improve simulations in the land surface model and the weather and climate model.

There are some operational networks of in situ SM measurement that have been established and maintained for long-term SM measurements. These networks include the Soil Climate Analysis Network, the Oklahoma Mesonet, and the Illinois Soil Water Survey in the US, as well as networks in the former Soviet Union and some Asia countries, and networks supported by scientific research programs. These networks provide valuable distributed

X. Shi · J. Wen (✉) · L. Wang · T. Zhang · H. Tian ·
X. Wang · R. Liu · J. Zhang
Laboratory for Climate Environment and Disasters of Western
China, Cold and Arid Regions Environmental and Engineering
Research Institute, Chinese Academy of Sciences,
320# Donggang West Road, Lanzhou 730000,
Gansu, People's Republic of China
e-mail: jwen@lzb.ac.cn

point measurements, but they are insufficient to characterize the spatial and temporal variability of SM at large scales (Njoku et al. 2003). There are also the low-resolution reanalysis SM datasets, such as the reanalysis datasets from the American National Centers for Environmental Prediction (NCEP) and European Centre for Medium-range Weather Forecast (ECMWF). These datasets usually have low resolutions and are generally used as model initial fields.

Today, satellite remote sensing observations provide an integrated global SM monitoring capability, and are effective in overcoming the shortcomings of the traditional methods. Compared to older optical remote sensors, which are sensitive to land surface reflectance and land surface temperature, the newly developed satellite microwave sensors have great advantages in land surface SM retrieval. Furthermore, the satellite passive microwave radiometer can work in all weather conditions, regardless of the cloud conditions. With the launch of the scanning multichannel microwave radiometer (SMMR) aboard Seasat and Nimbus-7 in 1978, and later, other microwave radiometers such as the special sensor microwave/imager (SSM/I), and the tropical rainfall measuring mission/microwave imager (TRMM/TMI), satellite microwave remote sensing radiometers have greatly accelerated the process of SM retrieval on the regional scale (Gao et al. 2006; Vinnikov et al. 1999; Wen et al. 2005). Especially useful is the advanced microwave scanning radiometer-E (AMSR-E) of the earth observation system aboard the Aqua satellite launched on 4 May 2002, which measures radiation at six frequencies in the range 6.9–89 GHz, all dual polarized. Compared to the SSM/I, the AMSR-E's 6.9 and 10.6 GHz channels have much longer wavelengths, which have better penetration ability and are more sensitive to changes in the dielectric constant of soil.

Studies on SM algorithm development and validation were carried out before the launch of the AMSR-E (Jackson 1993; Koike et al. 2000; Njoku and Li 1999). The method developed by Njoku et al. (2003) and Njoku and Chan (2006) is based on polarization ratios, which effectively eliminate or minimize the effects of surface temperature, resulting in a quantity that is dependent primarily on SM and vegetation. Yan and Jin (2004) also developed an algorithm to retrieve land surface SM using the polarization ratio data without much knowledge of surface roughness, vegetation canopy and so on, but this method requires monthly polarization ratio data and the ground observations of monthly average SM at first. This method is appropriate for short periods because of its treatment of parameters as constants. Zhao et al. (2007) used this method to estimate the SM at the Anni station on the central Tibetan plateau; the results are satisfactory. In this paper, the method is revised to obtain SM in a region in the

northeast of the Tibetan plateau, and then the satellite-derived SM datasets are used to improve SM simulation. After the above steps, the satellite brightness temperature data can be used directly as a data source for model simulations.

The data assimilation method is commonly used to apply the SM estimated from satellite remote sensing to the numerical simulations. The SM estimated from satellite microwave remote sensing data includes some errors, such as inaccurate evaluations of soil type, surface roughness, and vegetation coverage. The data is also limited by satellite scanning time; therefore, the data cannot be applied directly. The SM information can easily be attained through simulations of land surface models, but it is too sensitive to the model structure and model parameters. Wei (1995) pointed out that the operational SM product can be estimated by combining satellite SM and numerically simulated SM. With the process of assimilation, the consequent SM datasets have higher spatial-time resolution and less error than data generated by just one way. The commonly used methods for assimilating land surface data are the four-dimensional variational method, Kalman filter method, and ensemble Kalman filter method, etc. (Caya et al. 2005; Crow and Wood 2003). These methods can yield precise results; however, they are all very complicated and require more computation time than the general interpolation methods for a region simulation. Hoke and Anthes (1976) designed a method called the Newtonian relaxation or nudging method for assimilating the observation data for initializing the numerical model (more detailed information about this method in Sect. [Methodology](#)). Paniconi et al. (2003) and Hurkmans et al. (2006) implemented this relatively simple data assimilation method in a relatively complex hydrological model. Nudging proved successful in improving the hydrological simulation results, and it introduces little computational cost.

The objective of this paper is to provide a simple approach to applying satellite microwave remote sensed brightness temperature data to the Weather Research and Forecasting (WRF) model to improve regional SM simulation. A brief description of the geophysical and meteorological characteristics of the study area and satellite remote sensing data are given in Sect. [“The study area and the datasets”](#). An algorithm developed by Yan and Jin (2004) is introduced for SM retrieval from the AMSR-E brightness temperature datasets. In Sect. [“Methodology”](#), a newly designed four-dimensional NR method for assimilating SM in the Noah land surface model is introduced. In Sect. [“Newtonian relaxation assimilation scheme”](#), the regional SM values estimated from satellite remote sensing data are verified using ground measurements. A comparison between the numerically simulated SM values with the assimilation procedure, the non-assimilation procedure and

direct insertion of the satellite estimated SM datasets as the initial background field procedure is presented in Sect. “Assimilating estimated soil moisture into the WRF simulations”. Discussion and conclusion comprise the last section.

The study area and the datasets

An eastern part of the Qinghai-Tibet Plateau with high average altitude and a typical continental plateau climate was chosen as the study area (Fig. 1a). Its harsh environment keeps human activity away and facilitates a few of the ground meteorology observations. The thermal dynamics of the plateau have a significant impact on the East Asian monsoon and the global weather/climate system (Wu et al. 2005). The use of satellite remote sensing data in the land surface SM simulation in this area can contribute to research on the effect of thermal dynamics effect on weather/climate variability in such an inaccessible but important area.

Figure 1b shows the land use classification of the study area that is the domain of the WRF simulation in this investigation. There are Qaidam basin desert and Kumtag desert areas in the northwest, Tengger desert in the northeast, and bushes and grass mixed areas surrounding

the deserts. The southeast of the study area is mostly grassland, with several lakes sparsely distributed. Among these lakes, Lake Qinghai, Lake Gyaring and Lake Ngoring are the bigger three.

The ground measurement datasets utilized in this study were taken at two sites. The first one is an ECH₂O SM meter installed in the grassland at the Maqu station (33.85°N, 102.57°E) in the water source region of the Yellow River; no precipitation observations are available at this site. The second site is the Tanglha station (33.07°N, 91.94°E), which is a boundary layer meteorology observation station near the Qinghai-Tibet railway. There are precipitation observations available from this site. Both sites provide 5 cm depth SM measurements. Considering the scale-match between in situ data and satellite remote sensing or model simulation data, these two observation stations were both established in flat and open topography areas to increase their regional representation and minimize the scale-match problem. These observation datasets will be used to verify the SM values estimated from satellite microwave remote sensing data and the assimilation results.

The satellite brightness temperature data used in this investigation are the AMSR-E L2A re-sampled product, with original resolution of 25 km (detailed information on this product is available on <http://nsidc.org/data/amsre/index.html>). The AMSR-E scans the study area twice a day. The ascending orbital observation data from about 14:00 Beijing Standard Time (BST) are used in this research, and the AMSR-E measured brightness temperature data for July 2008 are collected in this study.

The land surface model used in the SM simulations is the Noah land surface model based on the one developed at Oregon State University (Chen and Dudhia 2001) and coupled in the WRF model. The Noah land surface model calculates the SM values in four layers: 10, 30, 60 and 100 cm. In addition, the SM values of the NCEP (1° × 1°) reanalysis datasets consist of four layers after 2005: 0–10, 10–40, 40–100 and 100–200 cm. Because the NCEP datasets are not interpolated to the depth of the soil layers for the WRF model, and are usually directly used as initial fields in simulations, the SM estimated from the AMSR-E measured brightness temperature data will also be used directly in the top layer SM simulation in the WRF model.

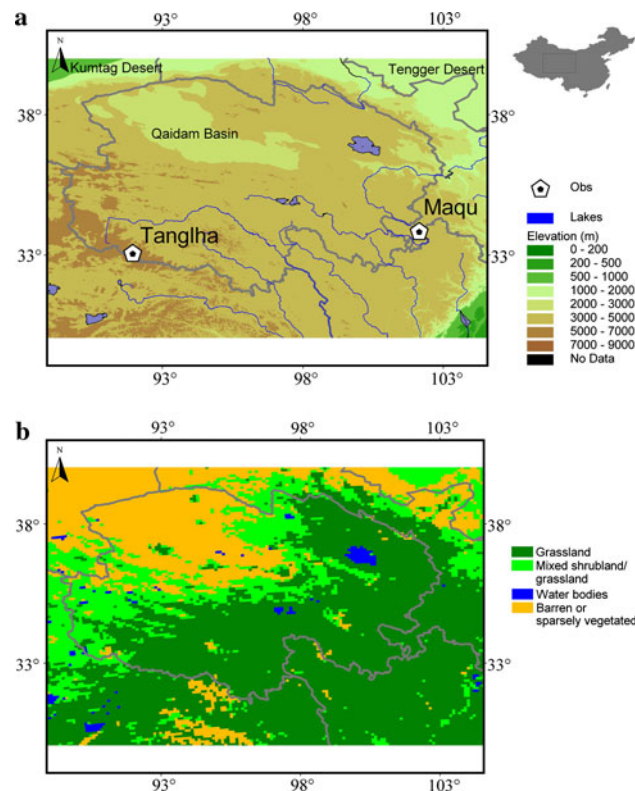


Fig. 1 Map of the study area combining with digital elevation model and observation sites (a), and the land use classification (b)

Methodology

Soil moisture estimates from satellite microwave remote sensing data

The dielectric constant mainly depends on the SM, and the complex dielectric constant of soil can be estimated from the study (Hallikainen et al. 1985). Assuming a smooth soil

surface and omitting bulk scattering, the microwave reflection indexes of the horizontal and vertical components of the soil surface (r_H, r_V) can be calculated with the Fresnel equation (Jackson et al. 2002; Ulaby et al. 1981). When the land surface roughness is taken into account, the microwave reflection indexes of the horizontal and vertical components (R_H, R_V) are modified:

$$R_H = [(1 - Q)r_H + Qr_V]e^{-h}, \quad (1)$$

$$R_V = [(1 - Q)r_V + Qr_H]e^{-h}, \quad (2)$$

where Q and h are the polarization ratio and the surface roughness parameter, respectively. In general $0 \leq Q < 0.5$. For the lower frequency (at 1.4 GHz), Q has a minimum effect on the surface SM calculation (Jackson 1993), and $Q = 0.174$ is used in this investigation (Njoku and Chan 2006).

The vector radiative transfer (VRT) equation for a uniform atmospheric layer and land surface with vegetation can be written as (Jin 1998)

$$T_{BP} = (1 - R_p)e^{-\tau}T_s + (1 - e^{-\tau})(1 + R_pe^{\tau})T_a, \quad (3)$$

where T_{BP} is brightness temperature, and P is either vertical (V) or horizontal (H) polarization. $\tau = \tau_a + \tau_v$ is the total opacity of the atmospheric layer and the vegetation layer. R_p is the polarized reflection index from Eq. 1 and/or Eq. 2. T_a and T_s are the average physical temperatures of the uniform atmospheric layer and land surface, respectively. Since T_a is generally smaller than T_s , it can be rewritten as $T_a = (1 - \delta_T)T_s$ with $0 \leq \delta_T \ll 1$. δ_T is defined as the air temperature parameter. In Eq. 3, the reflection of the top layer of vegetation and the scattering of the vegetation layer are ignored.

The microwave polarization difference index (MPDI) is commonly used to characterize the radiation brightness temperature difference between vertical and horizontal channels. From Eqs. 1–3, the MPDI can be rewritten and simplified:

$$\text{MPDI} \approx \frac{(R_H - R_V)(1 - 2Q)(1 + \delta_T)}{2e^{2\tau}e^h(1 - \delta_T) - (R_H + R_V)}. \quad (4)$$

The MPDI as defined in Eq. 4 is clearly dependent on the SM, the surface roughness parameter h , the atmospheric and vegetation opacity τ and the air temperature parameter δ_T . For example, increases in h , τ , Q , or $(1 - \delta_T)$ diminish the difference of the surface polarization radiation and hence decreases MPDI. On the other hand, increases in the SM boost ($R_H + R_V$) much more than $(R_H - R_V)$, and therefore yield a larger radiation difference and MPDI value. As previous equations have shown, $(R_H + R_V)$ and $(R_H - R_V)$ are functions of m_v , and are noted as R_+ and R_- for simplicity.

Statistically, parameters τ , Q , h , and δ_T of the same region in the same month should change little, so the variation of the MPDI reflects the change of the SM. In addition, when the SM varies from 0.05 (m^3/m^3) to 0.5 (m^3/m^3), $R_+(m_v)$ and $R_-(m_v)$ are from 0.2 to 1.0 and from 0.2 to 0.3, respectively. In this case, $R_-(m_v)$ closes to $R_{-<m_v>}$, that is $R_-(m_v)/R_{-<m_v>} \approx 1$, where $<m_v>$ is the monthly average of m_v (Yan and Jin 2004). With Eq. 4,

$$\begin{aligned} \frac{\text{MPDI}}{\langle \text{MPDI} \rangle} &\approx \frac{2e^{2\tau}e^h(1 - \delta_T) - R_+(<m_v>)}{2e^{2\tau}e^h(1 - \delta_T) - R_+(m_v)} \\ &\equiv \frac{a - R_+(<m_v>)}{a - R_+(m_v)}, \end{aligned} \quad (5)$$

where $a = 2e^{2\tau}e^h(1 - \delta_T)$, $\langle \text{MPDI} \rangle$ is the monthly average of MPDI. Given a , $\langle \text{MPDI} \rangle$ and $<m_v>$, the $R_+(m_v)$ can be derived from the current observation of MPDI, and the m_v can be found out by iteration.

As for parameter a , Yan and Jin (2004) treated it as constant, and determined it with two sets of known MPDI and m_v at different time. In our study, it is impossible to have two observations of any one grid point or to know the SM in advance. Therefore, τ and h were calculated based on previous algorithms (Meesters et al. 2005; Wang et al. 2006).

The above scheme accounts for the impact of soil type, surface roughness, and vegetation optical thickness in SM estimates. However, a key prerequisite is knowing the monthly average SM $<m_v>$ in advance, which is not an easy task considering that there are very limited records available for the whole Qinghai-Tibet Plateau. In order to provide the monthly average SM value for each grid point in the simulation area, we used the AMSR-E global monthly SM product (resolution $1^\circ \times 1^\circ$) as the $<m_v>$, and re-sampled it and the satellite remote sensing data to the 10 km resolution grids for further processing.

Newtonian relaxation assimilation scheme

In this study, the SM results estimated from satellite remote sensing data were assimilated into the Noah land surface model in WRF using the Newtonian relaxation (NR) assimilation scheme. This method was conducted adding a fake tendency term proportional to the difference between a simulated value and the observed value into one or several prediction (or forecast) equations. This makes the simulated value close to real observation and makes all variables balanced by the model dynamical framework in the entire nudging time. The NR results can be used as an initial field of forecast to improve the accuracy of prediction. Furthermore, multiple time observations can be

inserted into this initial field optimization process, and then the effective resolution of observation is raised (Hoke and Anthes 1976; Hurkmans et al. 2006).

The SM in the Noah land surface model is simulated through application of the diffusivity form of Richards equation, which can be formulated as follows

$$\frac{\partial m_v}{\partial t} = \frac{\partial}{\partial z} \left(D(m_v) \frac{\partial m_v}{\partial z} \right) + \frac{\partial K(m_v)}{\partial z} + S(m_v), \quad (6)$$

where K (m/s) is the hydraulic conductivity, D (m²/s) is the soil water diffusivity, S (m³/m³s) is representative for sinks and sources (i.e., rainfall, dew, evaporation and transpiration), t (s) is time, and m_v is the soil moisture. The non-linear $K - m_v$ and $D - m_v$ relationships are defined by the formulation of Cosby et al. (1984) for nine different soil types.

By adding a relaxation term on the right hand of Eq. 6, the assimilation equation is reformed as

$$\frac{\partial m_v}{\partial t} = \frac{\partial}{\partial z} \left(D(m_v) \frac{\partial m_v}{\partial z} \right) + \frac{\partial K(m_v)}{\partial z} + S(m_v) + G\omega(x, y, z, t)\varepsilon(x, y, z)(m_v^o - m_v), \quad (7)$$

where G denotes the strength of the relaxation interaction, which determines the relative value of the assimilation term with respect to all other physical forcing terms in this equation. G has dimension of s⁻¹ and accordingly has to be adjusted to match the slowest physical process in the equation. A prerequisite of G is to satisfy the stability criterion $G \leq 1/\Delta t$, where Δt is the nudging time of the analytical field. Generally, the simulation results are too close to observations and thus break the harmony of the fields if G is too big; or, if G is too small, the assimilation data plays no role in the simulation. Empirically, G varies in range 10⁻⁵–10⁻³ s⁻¹ and is usually set as 10⁻⁴ s⁻¹. $\omega(x, y, z, t)$ is the four-dimensional assimilation weighting function (at the temporal and spatial scales). $\varepsilon(x, y, z)$ is the quality factor of analytical value, is between 0 and 1.0, and relies on the data quality and distribution. m_v^o is the grid observation value from interpolating observations of neighbor times. In this study, only the first layer SM values were assimilated into the Noah land surface model. More details setting about G , ω and ε are explained in Sect. “Assimilating estimated soil moisture into the WRF simulations”. The nudging time for every observation data is 6 h in this study.

Analysis of the soil moisture estimated from AMSR-E

Evaluation of the estimated soil moisture

In this section, the SM estimations based on the above-mentioned theory are verified using ground observations

from 7 July 2008. No precipitation event occurred in this area during the study period, a favorite circumstance for linking the regional distribution of SM to the land use classification. It is also suitable for comparison between SM values from different sources. The average monthly AMSR-E SM of July for 2000–2007 was taken as the monthly SM of July 2008, due to lack of a monthly AMSR-E SM product at that time.

Figure 2a presents the regional distribution of the estimated SM with a 12 km spatial resolution based on the satellite brightness temperature. The regional distributions of the daily AMSR-E SM product, NCEP SM, are also provided (Fig. 2b, c) for the purpose of comparison. The estimated SM values in the desert areas ranged from 0.06 to 0.08 m³/m³, indicating a good correspondence between the estimated SM and the land use classification. In the bushes and grass mixed areas, the estimated SM values ranged from 0.04 to 0.08 m³/m³, slightly lower than actual observation and even dryer than the desert area in some cases. The estimated SM was about 0.08–0.22 m³/m³ in the grasslands and reaches a maximum in the Songpan grassland (about 32.00–34.00°N, 102.00–104.00°E), Sichuan province. We concluded that the regional distribution of the SM estimated from the satellite brightness temperature was acceptable.

Figure 2b presents the regional distribution of the daily AMSR-E SM product with a 25 km spatial resolution. The regional distribution pattern of the SM product was similar to that of the estimated SM in both the general tendency and the numerical values for each land use classification. The main differences were the SM distribution in the northwest desert area and the SM values in the southeast grassland. This product gave SM values ranging 0.06–0.10 m³/m³ for the northwest desert area, and the distribution of this SM product deviated from the distribution of the desert. In the grassland area, the SM values were slightly higher than the estimated SM values, and their distribution agreed better with the distribution of the grassland. However, another shortcoming of the product was that SM retrieval was not available for the Songpan grassland, where there was a large area of high SM values. In general, the difference values between the grassland and the desert were smaller in the SM product than that in the estimated SM.

Figure 2c is the regional distribution of the NCEP SM with a 1° × 1° spatial resolution. This is the background SM field of the Noah land surface model in this study. This product basically represents the characteristics of SM distribution in both desert and grassland. However, the SM in the desert areas, 0.10–0.20 m³/m³, was obviously too high. A field experiment was conducted in the Badain Jaran desert in 2008; the measured SM values were almost all less than 0.10 m³/m³. So, the values of the estimates and

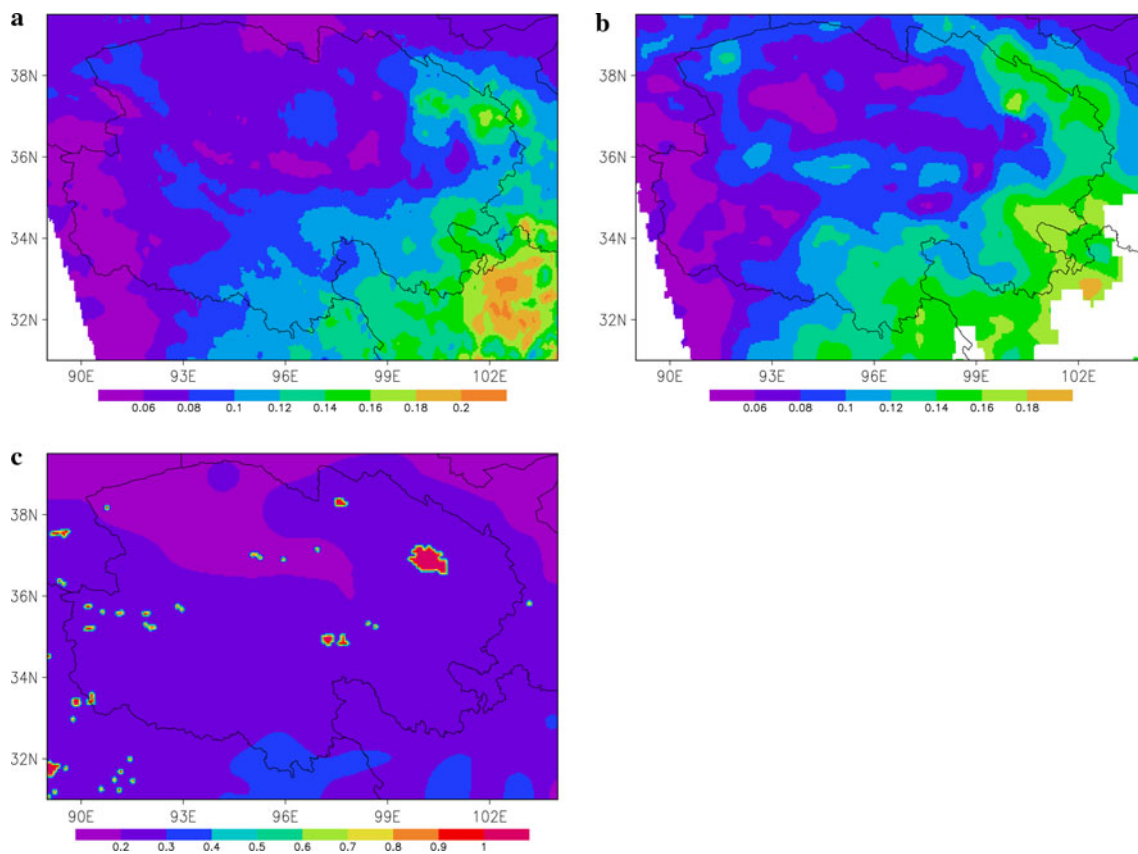


Fig. 2 Regional distribution of the estimated SM from AMSR-E brightness temperature data (a), the daily AMSR-E SM product (b), and the NCEP SM (c) at a 0–10 cm depth at 14:00 BST 7 July 2008

the AMSR-E SM products were better than that of the NCEP. The SM in bushes and grass mixed areas and grasslands were 0.20–0.25 and 0.25–0.30 m^3/m^3 , respectively. With reference to the available SM values in the literature, this product did not provide accurate information for bushes and grass mixed areas, and also missed the maximal SM area in the Songpan grassland due to its low resolution.

Verification of the soil moisture estimates

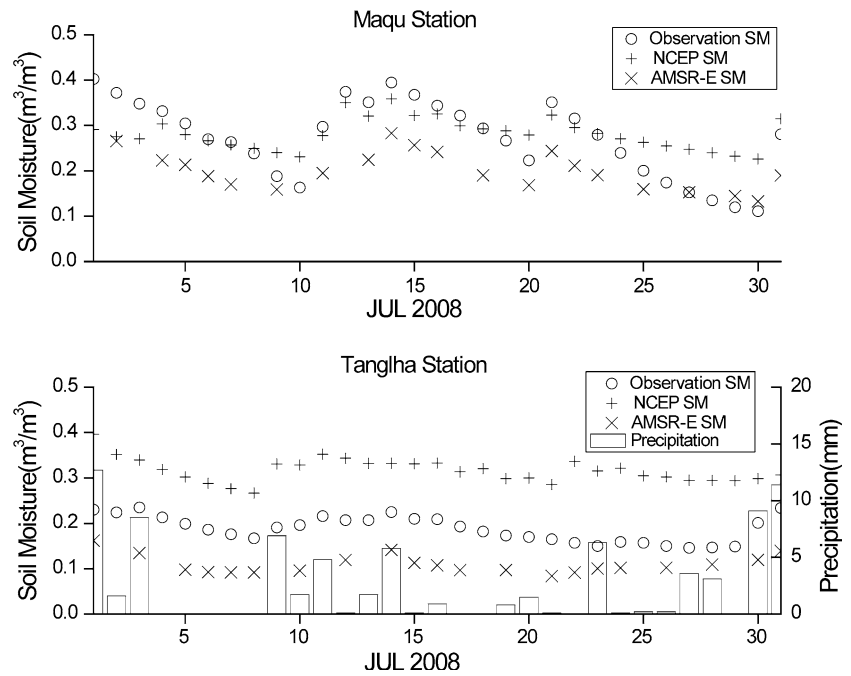
Before assimilating the satellite estimated SM into the Noah land surface model for simulating SM, the regional SM values estimated from the satellite microwave measured brightness temperature were verified by using 5 cm depth SM data collected in July 2008 at both the Maqu and Tanglha stations. The results are shown in Fig. 3.

The land surface type at the Maqu Station is grassland with a 3,512 m altitude. As Fig. 3a shows, the temporal variations of the satellite estimated SM and NCEP SM were highly correlated with the SM measured at this ground station. The three periods of decreasing SM in

1–10, 14–20 and 21–30 of July were clearly shown. As for the SM values, NCEP was closer to the ground observation than the values estimated from satellite measurements. However, the estimated SM provided better estimates of the low SM values than the NCEP SM did. The small amplitude of SM is another shortcoming of the NCEP data compared to the ground measurements.

The land surface type at the Tanglha Station is also grassland with a 5,100 m altitude. Figure 3b shows that the temporal variations of the estimated SM, the NCEP SM and the ground observations have similar trends. The NCEP SM provided much larger SM values than those of the ground observations, while the SM values estimated from satellite microwave measurement yielded smaller results than the ground observations. The estimated SM had less error than the NCEP SM. Gruhier et al. (2008) pointed out that the daily AMSR-E SM product cannot provide accurate SM values at the current stage, but it can provide reliable information on the land surface SM variation on a seasonal scale and for precipitation events. Considering analysis of the precipitation in July at the Tanglha Station, the SM estimated from AMSR-E brightness temperature presented

Fig. 3 Temporal variations of estimated SM from satellite microwave remote sensing data, NCEP SM at 0–10 cm depth and field observation at a 5 cm depth at the Maqu Station (a) and Tanglha Station (b)



a strong correspondence. For example, after precipitations events on 14, 24 and 30 of July, the SM estimated from AMSR-E data revealed a more clearly increasing trend than the NCEP SM.

Based on the previous comparison, it is clear that the SM estimated from the AMSR-E data is smaller than that of the ground observations. Beyond the inevitable errors in describing soil type, surface roughness, vegetation optical thickness and even SM heterogeneity, a possible reason is that the monthly average SM from the AMSR-E monthly SM product for July was insufficiently accurate. An accurate average monthly SM is essential for more accurate estimated SM values. Fortunately, the Soil Moisture and Ocean Salinity Mission (SMOS: see <http://smos.cnes.fr/SMOS/>) will be launched in the near future, and is equipped with an L-band (1.4 GHz) passive microwave radiometer. This radiometer is highly sensitive to land surface SM, and could provide more precise average monthly SM values.

Assimilating estimated soil moisture into the WRF simulations

The accuracy of a numerical model simulation or forecasting depends not only on the model itself, but also on the quality of the initial variable fields. In this section, the NR method is deployed to assimilate the SM estimated from AMSR-E data into the Noah land surface model in WRF, and the characteristics of the regional and temporal

patterns of SM are analyzed with the results of the numerical simulations.

Regional distribution of assimilated soil moisture

From the analysis in the Sect. “[Analysis of the soil moisture estimated from AMSR-E](#)”, it is clear that the estimated SM and NCEP SM have the same temporal trends, but different values in the regional distribution. These differences are mainly in the following areas: (1) the NCEP SM values were higher for desert areas; (2) the SM values estimated from satellite measurements were lower for bushes and grass mixed zones. So the quality factor for the NR method was set according to the land use category instead of the usual setting of 1.0. The best way to set quality factor values is to use the statistical errors between the actual SM values and the estimated SM values. However, these statistical errors cannot be determined in a short period of time due to the lack of actual SM measurements on the Qinghai-Tibet Plateau. So if the land use category was not desert and the estimated SM values were less than $0.05 \text{ m}^3/\text{m}^3$, then the quality factor was set to 0.5 at this grid; if the land use category was not desert and the estimated SM values were between 0.05 and $0.1 \text{ m}^3/\text{m}^3$, then the quality factor was set to 0.8 at this grid; the quality factor was set to 1.0 for other cases. The four-dimensional assimilation weighting function was set to 1.0, meaning that there was no influence on any other points or times when the estimated SM data were assimilated into the model. The relaxing strength factor was set to 0.00037 s^{-1}

for the entire grid. Tests show that these settings produce good simulation results for this study area.

In this paper, three nested domains were used in the WRF model for simulating SM distribution. Of these three domains, the third one was the smallest and had the highest resolution, with a 10 km grid spacing. This domain provided more detail on atmospheric force fields and land use categories for the Noah land surface model. Similarly, the Noah land surface model could produce better water and heat fields to feed to the WRF model as the bottom boundary conditions. The assimilation of the estimated SM was conducted only in the third domain. Because there are few ground observation stations in the research area, it is hard to verify which method yields better SM development; so the estimated SM at 7 July 14:00 BST was used for the assimilation test, and the simulation result was verified by land use category. The whole simulating period covered 02:00–14:00 BST 7 July, 02:00–08:00 BST was period for the model spin-up time, and 08:00–14:00 BST was the model assimilation time.

Figure 4 is the simulated regional distribution of SM with assimilated test and non-assimilated test. Simulated SM

values in the assimilated test decreased throughout almost the entire research area. Changes in SM values in the desert areas and bushes/grass mixed zones ranged from -0.02 to -0.04 m^3/m^3 and -0.04 to -0.06 m^3/m^3 , respectively. In the assimilation test, the simulated desert SM values in the Qaidam basin located in the north Qinghai-Tibet Plateau, were between 0.1 and 0.15 m^3/m^3 , and demonstrated better agreement with the distribution of desert areas than non-assimilated test. This result also occurred in the Tengger desert area. In southern Qinghai province (95 – 97°E , 31 – 33°N), the simulated SM values obviously decrease, with a good correspondence to a small bare-ground tundra zone. In southwestern Qinghai province (90 – 93°E , 31 – 34°N), the simulated SM values also obviously decreased in small bushes and grass mixed zones. In addition, the simulated SM values showed almost no change if the SM estimated from satellite measurements were absent.

In summary, it can be concluded that after assimilating the estimated SM values using the NR method, the regional distribution of the simulated SM values improved most in desert areas, followed by grass and bushes and grass mixed zones.

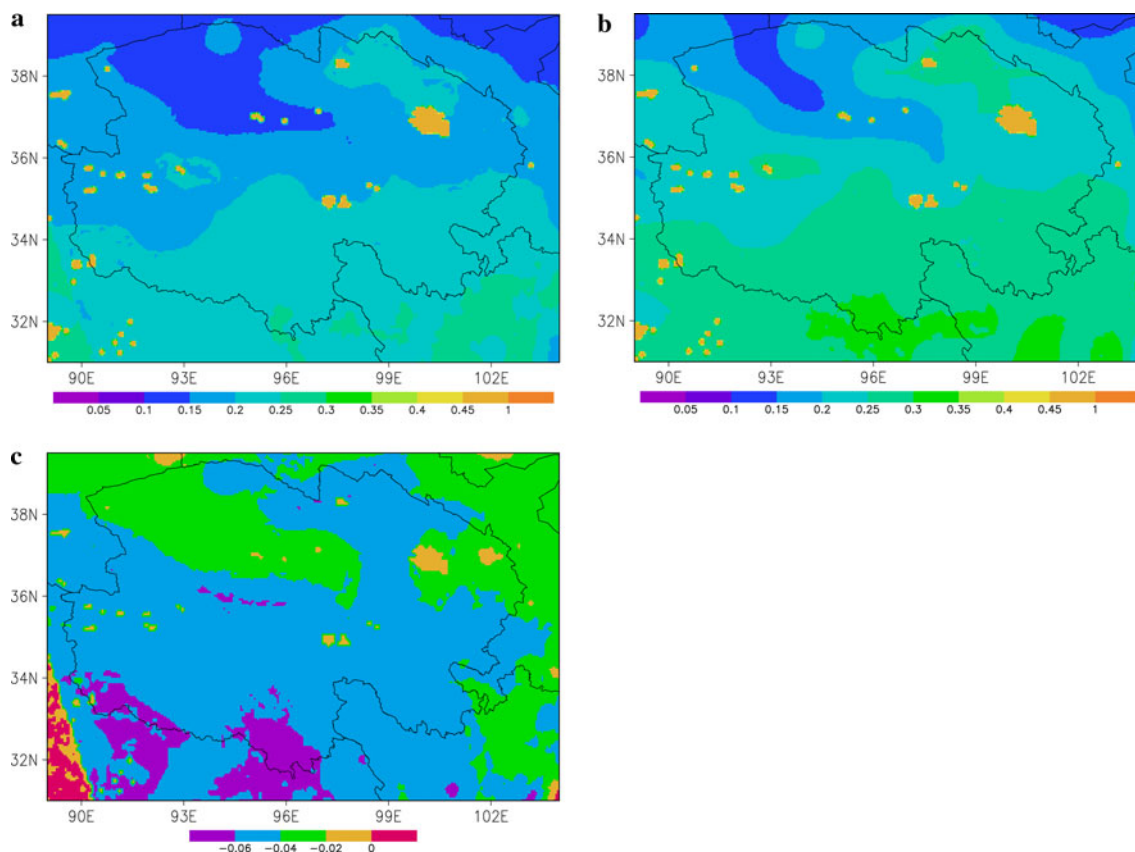


Fig. 4 Regional distribution of simulated soil moisture with assimilation (a), non-assimilation (b), and their discrepancy (c) at 14:00 BST 7 July 2008

Temporal variation of the assimilated soil moisture values

On a temporal scale, the objective of the assimilation procedure is to syncretize the variation of the SM estimated from satellite microwave measurement to the background SM field of a numerical model, and make the simulated SM values approach the ground observations to improve the long-term simulation results of the numerical model.

In this section, three tests were applied to measure the influence of the assimilation methods for the WRF simulations. The first test used the Newtonian relaxation method (NR); the direct insertion method was used in the second test (DI); and the third test used no assimilation step (NO). The simulated results were verified by the data collected from the Maqu Station and the Tanglha Station, as shown in Fig. 5. The simulation and assimilation parameters in the three tests were set as described in Sect. “Regional distribution of assimilated soil moisture”. The simulation period spanned 14 days from 14:00 BST on 17 July to 14:00 BST on 31 July. The lateral boundary conditions were updated every 6 h, same as the output frequency of the simulation. The assimilating period was from 08:00 to 14:00 BST for NR each day, and at 14:00 BST for the DI method each day. In addition, the root mean square error (RMSE) was used to evaluate the simulation results:

$$RMSE = \sqrt{\frac{1}{N} \sum_{t=1}^N (Obs_t - X_t)^2}, \tag{8}$$

where N is the entire simulation period, Obs_t is the ground observation at time t , X_t is the simulated value at the same time.

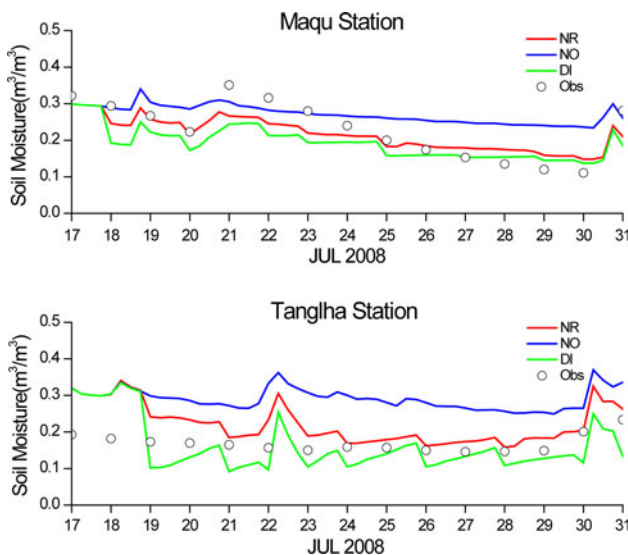


Fig. 5 Temporal variability of the ground-measured and simulated SM at the Maqu Station (a), and the Tanglha Station (b) from 17 to 31 July 2008

The simulated SM at the Maqu Station for the three methods is presented in Fig. 5a. The NO method showed little variation in SM throughout the entire simulation period. It did not reflect the significant variation in actual SM values, especially on 21 and 31 of July. Although the temporal variation of the estimated SM was assimilated in the DI scheme, there were still some errors in the SM estimated from satellite brightness temperature that led to inaccurate simulation results, especially for 18–23 July. Considering the temporal variation of the estimated SM, the temporal variation of the simulated SM using the NR method was revealed. It not only reflected significant SM variation on 21 and 31 of July, but also had less error than the DI method for 18–23 July. The RMSE of NO, DI and NR at this station were 0.07, 0.06 and 0.04 m³/m³, respectively, and the NR scheme provided the best estimation of these three methods.

The SM simulation at the Tanglha Station (Fig. 5b) was similar to at the simulation at the Maqu Station. The simulated SM values with the NO scheme were much larger than the actual values throughout the simulation period. The simulated SM values for the DI scheme were too small. The simulated SM values with the NR method were much closer to the ground measurements. The RMSE of NO, DI and NR at this station were 0.12, 0.07 and 0.05 m³/m³, respectively. Because there was an obvious difference between the NCEP and the estimated SM in this station, and the data input frequency for the NCEP data was four times that of the estimated SM, the simulated SM showed an upward trend at the non-assimilation time, and the correlation coefficient between the simulated SM and the station SM decreased. So if the model background SM was more divergent from the estimated SM, the variation tendency of simulated SM has been changed at the temporal scale. Furthermore, the DI method, compared with the NR method, produced a larger discrepancy from the numerical model at the temporal scale.

In conclusion, the best simulation results were achieved by assimilating the estimated SM with the NR method. The simulated SM finally tended toward the ground observations step by step, and the temporal characteristics of simulated SM were disclosed. This is helpful for the WRF model to improve the simulation accuracy of SM in rainfall events and seasonal variations.

Discussion and conclusion

In this paper, we analyzed the potential of using satellite microwave bright temperature data to improve the performance of numerical simulations of SM. The SM estimated from AMSR-E microwave bright temperature data were assimilated into the Noah land surface model in WRF by the NR method. The main conclusions are as follows:

1. Based on the theory of Yan and Jin (2004), regional SM values in the eastern part of the Qinghai-Tibet Plateau were estimated from AMSR-E brightness temperature data. Results showed that the estimated SM values were lower than the observation data at the two stations but within the bounds of common sense. Compared with the NCEP SM data, the estimated SM values showed a better response to daily precipitation. In addition, the distribution patterns of estimated SM were somewhat better than those from the AMSR-E daily products over this region.

2. Comparing the simulation results with the NO and DI methods, the NR method showed to be more accurate in simulating SM variation in the WRF model. At the regional scale, the model-simulated SM values improved most in the desert areas, and then the grasslands and bushes and grass mixed zones. At the temporal scale, the RMSE between the simulated SM and ground-measured SM decreased 0.03 and 0.07 m³/m³ using the NR method at the Maqu Station and the Tanglha Station, respectively.

The limitation of the NR method is that its parameter settings need an experience. In this study, the quality factor was set according to the land use category and the estimated SM, and the four-dimensional assimilation weighting function was set to 1.0. Hurkmans et al. (2006) designed three empirical functions for setting the four-dimensional assimilation weighting function. This method is a good try, but it needs further verification in different regions.

In addition, there is concern about the direct insertion of SM estimated from satellite remote sensing measurements into numerical models. Ookouchi et al. (1984) mentioned that sharp horizontal SM gradients may generate thermal circulations as strong as sea breezes, and thus may trigger convection. Considering the constraints of the satellite scanning region, if the DI method is deployed to assimilate estimated SM, then this can easily lead to sharp horizontal soil moisture gradients between estimated SM and simulated SM at the intersection border. This kind of gradient has a negative effect on the WRF model's capacity to simulate convection for producing more fake precipitation near the intersection border. The NR method could weaken this sharp horizontal SM gradient through a period of nudging assimilation.

Acknowledgments This work was supported by the National Science Foundation of China (Grant No. 40775022) and the Innovation Project of the Chinese Academy of Sciences (KZCX2-YW-328). The authors would like to thank the Tanglha Station and the Maqu Station of the Cold and Arid Regions Environmental and Engineering Research Institute, Chinese Academy of Sciences, for providing the soil moisture and precipitation datasets. Two anonymous reviewers are gratefully acknowledged for their comments and suggestions.

References

- Caya A, Sun J, Snyder C (2005) A comparison between the 4DVAR and the ensemble Kalman filter techniques for radar data assimilation. *Mon Weather Rev* 133:3081–3094
- Chen F, Dudhia J (2001) Coupling an advanced land-surface/hydrology model with the Penn State/NCAR MM5 modeling system, Part I: model description and implementation. *Mon Weather Rev* 129(4):569–585
- Clark CA, Arritt RW (1995) Numerical simulations of the effect of soil moisture and vegetation cover on the development of deep convection. *J Appl Meteorol* 34:2029–2045
- Cosby BJ, Hornberger GM, Clapp RB, Ginn TR (1984) A statistical exploration of the relationships of soil moisture characteristics to the physical properties of soils. *Water Resour Res* 20(6):682–690
- Crow WT, Wood EF (2003) The assimilation of remotely sensed soil brightness temperature imagery into a land surface model using ensemble Kalman filtering: a case study based on ESTAR measurements during SGP97. *Adv Water Resour* 26:137–149
- Gallus WA Jr, Segal M (2000) Sensitivity of forecast rainfall in a Texas convective system to soil moisture and convective parameterization. *Weather Forecast* 15:509–525
- Gao H, Wood EF, Jackson TJ, Drusch M (2006) Using TRMM/TMI to retrieve surface soil moisture over the southern United States from 1998 to 2002. *J Hydrometeorol* 7(1):23–38
- Gruhier C, Rosnay PD, Kerr Y, Mougin E, Ceschia E, Calvet J-C, Richaume P (2008) Evaluation of AMSR-E soil moisture product based on ground measurements over temperate and semi-arid regions. *Geophys Res Lett* 35:L10405. doi:10.11029/12008GL033330
- Hallikainen MT, Ulaby FT, Dobson MC, El-Rayes MA (1985) Microwave dielectric behavior of wet soil-part I: empirical models and experimental observations. *IEEE Trans Geosci Remote Sens* GE-23(1):25–34
- Hoke J, Anthes R (1976) The initialization of numerical models by a dynamic relaxation technique. *Mon Weather Rev* 104:1551–1556
- Hurkmans R, Paniconi C, Troch PA (2006) Numerical assessment of a dynamical relaxation data assimilation scheme for a catchment hydrological model. *Hydrol Process* 20(3):549–563
- Jackson TJ (1993) Measuring surface soil moisture using passive microwave remote sensing. *Hydrol Process* 7(2):139–152
- Jackson TJ, Hsu AY, O'Neill PE (2002) Surface soil moisture retrieval and mapping using high-frequency microwave satellite observation in the southern great plain. *J Hydrometeorol* 3:688–699
- Jin Y-Q (1998) Monitoring regional sea ice of China's Bohai Sea by SSM/I scattering indexes. *IEEE J Ocean Eng* 23(2):141–144
- Koike T, Fujii H, Tamagawa K (2000) Development and validation of microwave radiometer algorithms for land surface hydrology. *Int Symp Remote Sens, Kyongju, Korea*, pp 503–508
- Meesters AGCA, Jeu RAMD, Owe M (2005) Analytical derivation of the vegetation optical depth from the microwave polarization difference index. *IEEE Geosci Remote Sens Lett* 2(2):121–123
- Njoku EG, Chan SK (2006) Vegetation and surface roughness effects on AMSR-E land observations. *Remote Sens Environ* 100(2):190–199
- Njoku EG, Li L (1999) Retrieval of land surface parameters using passive microwave measurements at 6–18 GHz. *IEEE Trans Geosci Remote Sens* 37(1):79–92
- Njoku EG, Jackson TJ, Lakshmi V, Chan TK, Nghiem SV (2003) Soil moisture retrieval from AMSR-E. *IEEE Trans Geosci Remote Sens* 41(2):215–229
- Ookouchi Y, Segal M, Kessler RC, Piekle RA (1984) Evaluation of soil moisture effects on generation and modification of meso-scale circulations. *Mon Weather Rev* 112:2281–2292

- Paniconi C, Marrocu M, Putti M, Verbunt M (2003) Newtonian nudging for a Richards equation-based distributed hydrological model. *Adv Water Resour* 26:161–178
- Prigent C, Aires F, Rossow WB, Robock A (2005) Sensitivity of satellite microwave and infrared observation to soil moisture at a global scale: relationship of satellite observations to in situ soil moisture measurements. *J Geophys Res* 110:D07110. doi: [07110.1029/2004JD005087](https://doi.org/10.1029/2004JD005087)
- Ulaby FT, Moore RK, Fung AK (1981) Microwave remote sensing: active and passive. Vol. 1: microwave remote sensing fundamentals and radiometry. Addison-Wesley, Reading, MA, pp 456
- Vinnikov KY, Yezzerkepova IB (1991) Soil moisture: empirical data and model results. *J Clim* 4(1):66–79
- Vinnikov KY, Robock A, Qiu S, Entin JK (1999) Satellite remote sensing of soil moisture in Illinois, United States. *J Geophys Res* 104(D4):4145–4168
- Wagner W, Scipal K, Pathe C, Gerten D, Lucht W, Rudolf B (2003) Evaluation of the agreement between the first global remotely sensed soil moisture data with model and precipitation data. *J Geophys Res* 108(D19):4611. doi: [4610.1029/2003JD003663](https://doi.org/10.1029/2003JD003663)
- Wang L, Li Z, Chen Q (2006) New calibration method for soil roughness parameters with AMSR-E observations. *J Remote Sens* 10(10):654–660 (in Chinese)
- Wei M-Y (1995) Soil moisture: report of a workshop held in Tiburon, California, 25–27 January 1994, NASA Conf Publ 3319, pp 80
- Wen J, Jackson TJ, Bindlish R (2005) Retrieval of soil moisture and vegetation water content using SSM/I data over a corn and soybean region. *J Hydrometeorol* 6(6):854–863
- Wu G-X, Liu Y-M, Liu X, Duan A-M, Liang X-Y (2005) How the heating over the Tibetan plateau affects the Asian climate in summer. *J Atmos Sci* 29(1):47–56 (in Chinese)
- Yan FH, Jin YQ (2004) Statistics of the average distance of polarization index derived from data of space-borne microwave remote sensing and soil moisture mapping. *J Radio Sci* 19(4):386–392 (in Chinese)
- Zhao YZ, Ma YM, Huang Z, Yuan T (2007) The retrieval of soil moisture from TRMM/TMI data in central of Tibetan plateau. *Plateau Meteorol* 26(5):952–957 (in Chinese)